JOURNAL OF CATALYSIS **166,** 218–228 (1997)
ARTICLE NO. CA971551

In Situ Controlled Promotion of Catalyst Surfaces via NEMCA: The Effect of Na on the Pt-Catalyzed NO Reduction by H_2

O. A. Marina,*[,1] I. V. Yentekakis,* C. G. Vayenas,*[,2] A. Palermo,†[,3] and R. M. Lambert†

*Department of Chemical Engineering, University of Patras, GR-26500 Patras, Greece; and †Department of Chemistry, Cambridge University, Cambridge CB2 1EW, England

Received April 17, 1996; revised November 11, 1996; accepted December 2, 1996

It was found that the catalytic activity and selectivity of Pt for NO reduction by H_2 can be markedly and reversibly affected by depositing polycrystalline Pt films on β''-Al_2O_3, a Na^+ conductor, and applying external currents or potentials to supply or remove Na to or from the Pt catalyst surface. The increase in the rate of NO reduction to N_2 is typically 10^3–10^5 times larger than the rate of supply of Na and up to 30 times larger than the umpromoted rate. The use of the β''-Al_2O_3 support permits precise *in situ* control of the Na coverage on the Pt surface. Sodium coverages of 0.06 cause up to 1450% increases in the total rate of NO reduction and enhance the selectivity to N_2 from 30 to 75%. The promotional effect of Na is due to enhanced NO chemisorption and dissociation on the Pt surface.

INTRODUCTION

The effect of non-Faradaic electrochemical modification of catalytic activity (NEMCA) (1–9) or electrochemical promotion (10, 11) or *in situ* controlled promotion (12, 13) has been studied for over 40 catalytic reactions of Pt, Pd, Rh, Au, Ag, Ni, and IrO_2 surfaces. Work in this area has been extensively reviewed. (14–17). In brief it has been found that the catalytic (1–17) and chemisorptive (18, 19) properties of polycrystalline metal films interfaced with solid electrolytes, such as yttria-stabilized zirconia (YSZ), an O^{2-} conductor, β''-Al_2O_3, a Na^+ conductor, CaF_2, a F^- conductor, or TiO_2, a mixed electronic–ionic conductor, can be affected dramatically and reversibly by electrically polarizing the metal–solid electrolyte interface. More recently the effect has been demonstrated using protonic conductors (20, 21) and aqueous alkaline solutions (22).

A potentially important application of electrochemical promotion is in enhancing the catalytic activity and selectivity of metals for the reduction NO to N_2, a reaction of great technological and environmental interest. It was recently found that the use of β''-Al_2O_3 to reversibly dose Na on Pt leads to very significant enhancement in the rate and N_2 selectivity of the Pt-catalyzed NO reduction by CO (23–25), C_2H_4 (11), and C_3H_6 (24, 25). The present paper is a logical extension of our work on the electrochemical promotion of environmentally important catalytic reactions. The use of hydrogen as a reducing agent for NO has been discussed in the literature for about 20 years; the process is also of importance in automotive catalysts (26). One of the key issues is the relatively poor selectivity of many catalysts which tend to produce substantial amounts of N_2O and, worse, NH_3. Recently, there has been renewed interest in the NO/H_2 reaction as a result of improved selectivity exhibited by Pd and Pd/Mo on alumina catalysts (27, 28). Our results demonstrate that Na promotion greatly enhances both the activity and the selectivity for N_2 production.

Platinum group metals are used widely for the catalytic removal of NO from effluent gases by means of NO reduction with light hydrocarbons, H_2, NH_3, or CO. Because of its ability to chemisorb NO dissociatively Rh is in general the most active and selective catalyst for NO reduction (29). Due to its scarcity, increased Rh replacement by Pt in automotive exhaust catalytic converters is generally considered desirable (30) despite recent fluctuations in the relative market supply of noble metals.

The activity and selectivity of the $NO + H_2$ reaction on Pt surfaces is largely determined by the nature of the adsorbed states (molecular or dissociative NO chemisorption) which is strongly dependent on surface structure (31). Both supported Pt catalysts and polycrystalline Pt wires and foils exhibit a low activity for NO dissociation because after high temperature treatment ($T > 300°C$) their surfaces consist predominantly of Pt(111) and hex-Pt(100) crystal planes which adsorb NO only molecularly (32, 33).

Alkali metals exhibit a strong promotional effect for NO dissociation on transition metal surfaces (34). Nevertheless, the subject has been essentially overlooked in regard to practical NO_x reduction catalysts. Our work serves to underline the surprisingly neglected opportunities for NO_x

[1] Present address: Boreskov Institute of Catalysis, Novosibirsk 630090, Russia.

[2] To whom correspondence should be addressed.

[3] Present address: INTEMA-CONICET, Universidad Nac. Mar del Plata 7600, Mar del Plata, Argentina.

0021-9517/97 $25.00

reduction offered by Na promotion of Pt metals. In addition, the electrochemical technique enables us to probe the effects of promoter addition in a unique and controllable way that provides useful insight into the reaction mechanism. Sodium, in particular, can be deposited on Pt surfaces either from the gas phase by dosing from an evaporation source or by interfacing the catalyst film with a Na^+-conducting solid electrolyte, such as β''-Al_2O_3 (3, 5, 11, 12, 23–25, 35). In the latter case by appropriate voltage application (± 1 V) one can control, *in situ*, the coverage of the alkaline promoter on the active metal surface. This has been recently confirmed by a variety of techniques including work function measurements (3), X-ray photoelectron spectroscopy (XPS), (24, 25, 36), and scanning tunneling microscopy (STM) (37).

It is worth noting that a similar approach employing borosilicate glasses, instead of solid electrolytes, and very large applied potentials (± 5–10 kV) has been explored to control the coverage of Na on semiconductor catalysts such as TiO_2 and ZnO (38, 39).

EXPERIMENTAL

The experiments were carried out in a continuous flow well-mixed "single-pellet" type reactor described previously (6, 12) (Fig. 1) The β''-Al_2O_3 disc was suspended in the quartz reactor with the three electrodes (catalyst, counter, and reference), all exposed to the reacting gas mixture. The reactor volume was 25 cm^3.

The Pt catalyst film was deposited on one side of the β''-Al_2O_3 disc (Ceramatec) following the method described previously (12–14), i.e., by using a thin coating of Engelhard Pt A1121 paste followed by calcination in air first at 400°C for 1 h and then at 750°C for 20 min. The true surface area of the Pt catalyst was determined via the isothermal surface titration technique described in detail elsewhere (14, 16). The reactive oxygen uptake, N_O, of the catalyst at 375°C obtained via isothermal oxygen titration with CO (12, 14) was 3.8×10^{-7} mol O, which corresponds (12, 14) to 150 cm^2. Figure 2 shows the isothermal oxygen titration results, i.e., it depicts the amount, N, of previously adsorbed reactive oxygen (forming CO_2 after exposure to CO) remaining on the surface after isothermal desorption in ultrapure He for various times t_{He}. N_O is determined by extrapolation to $t_{He} = 0$ (12, 14, 16). The triangle on the same figure shows the value of N_O estimated from the literature value of the initial dipole moment of Na on Pt(111) in conjunction with Helmholz's equation (12) as described below. This estimate is a factor of 2 smaller than the value obtained via surface titration.

The Au counter and reference electrodes were deposited on the other side of the β''-Al_2O_3 disk (Fig. 1) using Demetron M8032 Au paste followed by calcination at 750°C. Blank experiments performed with the Au catalyst

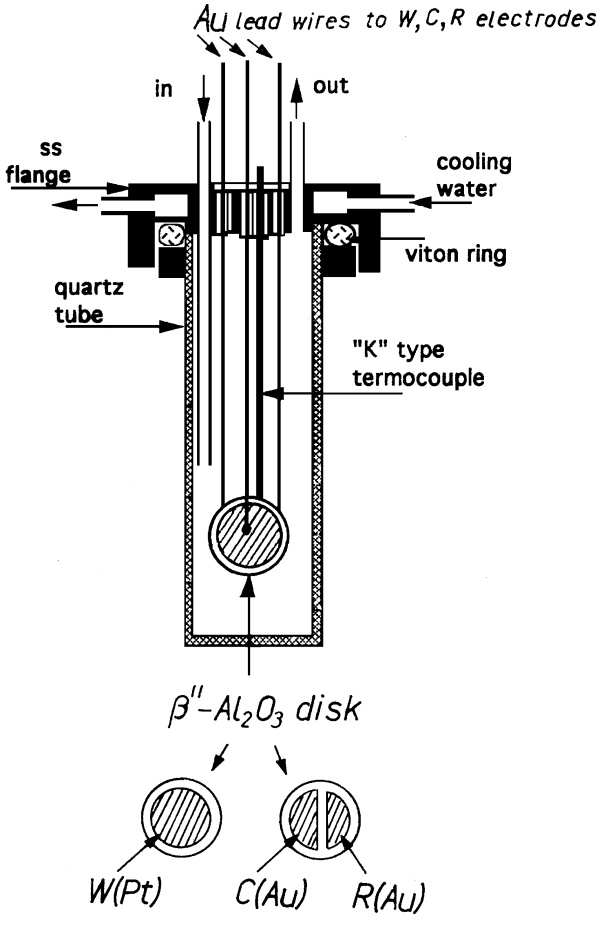

FIG. 1. Single pellet reactor and electrode configuration.

film and Au reference and counter electrodes under the same experimental conditions have shown that Au, which does not adsorb NO and H_2 dissociatively, is catalytically inert for the $NO + H_2$ reaction. Thus all the current- and potential-induced changes in catalytic activity described below can be attributed to the Pt catalyst only.

Reactants were L' Air Liquide certified standards of 3% NO in He and 2% H_2 in He. They were further diluted in ultrapure He (99.999%) and were used without additional purification. Reactants and products were analyzed by online gas chromatography (Perkin-Elmer Sigma 2) with a TC detector. A Porapak Q column at 40°C was used to separate N_2O and a molecular sieve 5A column at 110°C was used to separate H_2, N_2, and NO. Nitrogen, nitrous oxide, and water were the only measurable products. Ammonia has also been reported as a product of the $NO–H_2$ reaction on polycrystalline Pt under reducing conditions (43). No ammonia was detected in the present work due to the relatively high NO/H_2 ratios used.

The kinetics of the reaction were studied at atmospheric pressure and over the temperature range 300–430°C. The NO partial pressure was varied between 0 and 1.6 kPa and

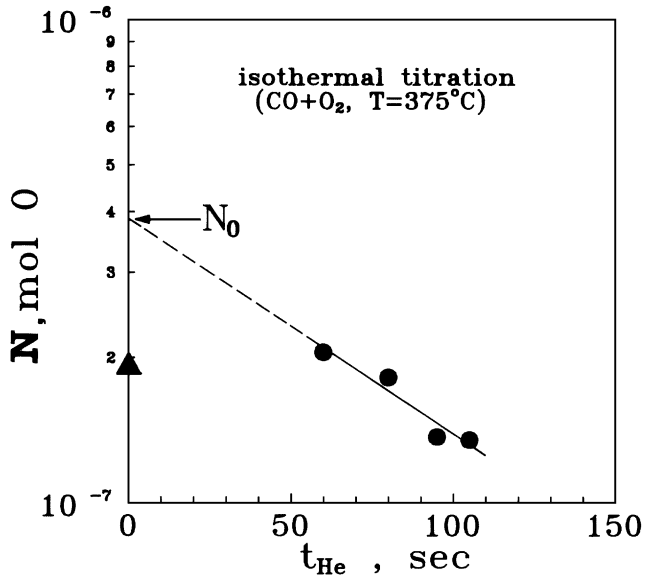

FIG. 2. Effect of desorption time t_{He} on the amount, N, of reactive oxygen adsorbed on the unpromoted Pt surface; N is measured by the total amount of CO_2 formed upon exposure to CO; the maximum oxygen reactive uptake, N_O, is obtained by extrapolating to $t_{He} = 0$. (▲) N_O value estimated on the basis of the initial dipole moment analysis; see text for discussion.

the H_2 partial pressure was varied between 0 and 1 kPa. The total gas flow rate was high, typically 300–600 cm^3/min in order to minimize the conversion of the reactants and to eliminate mass and heat transfer effects. The NO and H_2 conversions were also thus kept below 25 and 40%, respectively.

In order to clean the Pt catalyst surface from Na which inevitably migrates on the Pt surface from the β''-Al_2O_3 structure during sintering at 750°C, a potential difference $V_{WR} = +400$ mV was applied between the catalyst and reference electrodes at $T = 400$°C until the current ($I > 0$) between the catalyst and the counter electrode vanished. This current corresponds to the reaction

$$Na(Pt) \leftrightharpoons Na^+(\beta''\text{-}Al_2O_3) + e^-. \qquad [1]$$

Our recent XPS studies have demonstrated directly the reversible pumping of Na to/from beta″ alumina from/to the Pt catalyst (25). They have also shown that the Pt catalyst can indeed be entirely cleaned of Na by the application of a positive potential.

All results reported here were obtained in the potentiostatic mode of operation, i.e., by setting V_{WR} at constant values. Galvanostatic (constant current) operation was used only in the transient experiments.

RESULTS

Transient Effect of Applied Constant Current

Figure 3 shows a typical galvanostatic transient, i.e., it depicts the effect of applying a constant negative current (Na supply to the catalyst) on catalyst potential V_{WR}, and rates of N_2 and N_2O production. Figure 3a also shows a V_{WR} transient obtained in presence of He, when no catalytic reaction is taking place on the Pt catalyst.

The V_{WR} vs time transient shown in Fig. 3a is very similar to those obtained in previous electrochemical promotion studies of C_2H_4 (5, 35) and CO (12) oxidation and NO reduction by CO (23–25) on Pt/β''-Al_2O_3. These previous studies have established that the galvanostatic V_{WR} transients are very useful for two purposes:

I. Establishing the relationship between V_{WR} and Na coverage, θ_{Na}, under reaction conditions.

II. Obtaining information about the dipole moment, P_{Na}, of Na species on the catalyst surface under reaction conditions.

The analysis proceeds as follows: first the Na coverage is computed via Faraday's Law,

$$\theta_{Na} = -It/FN_O, \qquad [2]$$

where t is the time of current application I, F is Faraday's constant, and N_O is the number of available Pt sites (3.8×10^{-7} mol Pt) independently measured via surface titration (Fig. 2). This permits construction of the θ_{Na} abscissa in Fig. 3a. Thus the V_{WR} transient establishes the relationship $\theta_{Na}(V_{WR})$ between Na coverage and V_{WR}. (Fig. 4). This relationship is in general dependent on gaseous composition but the dependence is relatively weak (12) because the catalyst work function $e\Phi$ varies according to

$$e\Delta V_{WR} = \Delta(e\Phi) \qquad [3]$$

and is determined primarily by the coverage of Na, due to the large dipole moment of Na (~5 Debye) (12) on the Pt surface. The latter, P_{Na}, can be computed from the V_{WR} transient via the differentiated Helmholz equation (12, 16, 40–42),

$$\frac{ed V_{WR}}{dt} = \frac{d(e\Phi)}{dt} = \frac{P_{Na} \cdot I}{\varepsilon_o \cdot A}, \qquad [4]$$

where $\varepsilon_o = 8.85 \times 10^{-12}$ C^2/Jm and A is the Pt film surface area (1.5×10^{-2} m^2) computed from $N_O = 3.8 \times 10^{-7}$ mol Pt and the Pt(111) atom density, $d = 1.53 \times 10^{19}$ atoms/m^2.

Thus from the initial slope of the V_{WR} transient upon current application (Fig. 3a) one computes via Eq. [4] an initial dipole moment for Na, P^o_{Na}, of 3.7×10^{-29} C · m (11.2 Debye) which is a factor of two larger than the literature value (12) of 5.3 Debye for Na on clean Pt(111) and with the value of 5 ± 0.4 Debye extracted in previous electrochemical promotion studies on polycrystalline Pt films using the same approach (12). Alternatively by using the literature value of 5.3 Debye and the initial V_{WR} slope one can obtain an estimate of the catalyst surface area A and thus its reactive oxygen uptake N_O, as previously noted (Fig. 2). The computed

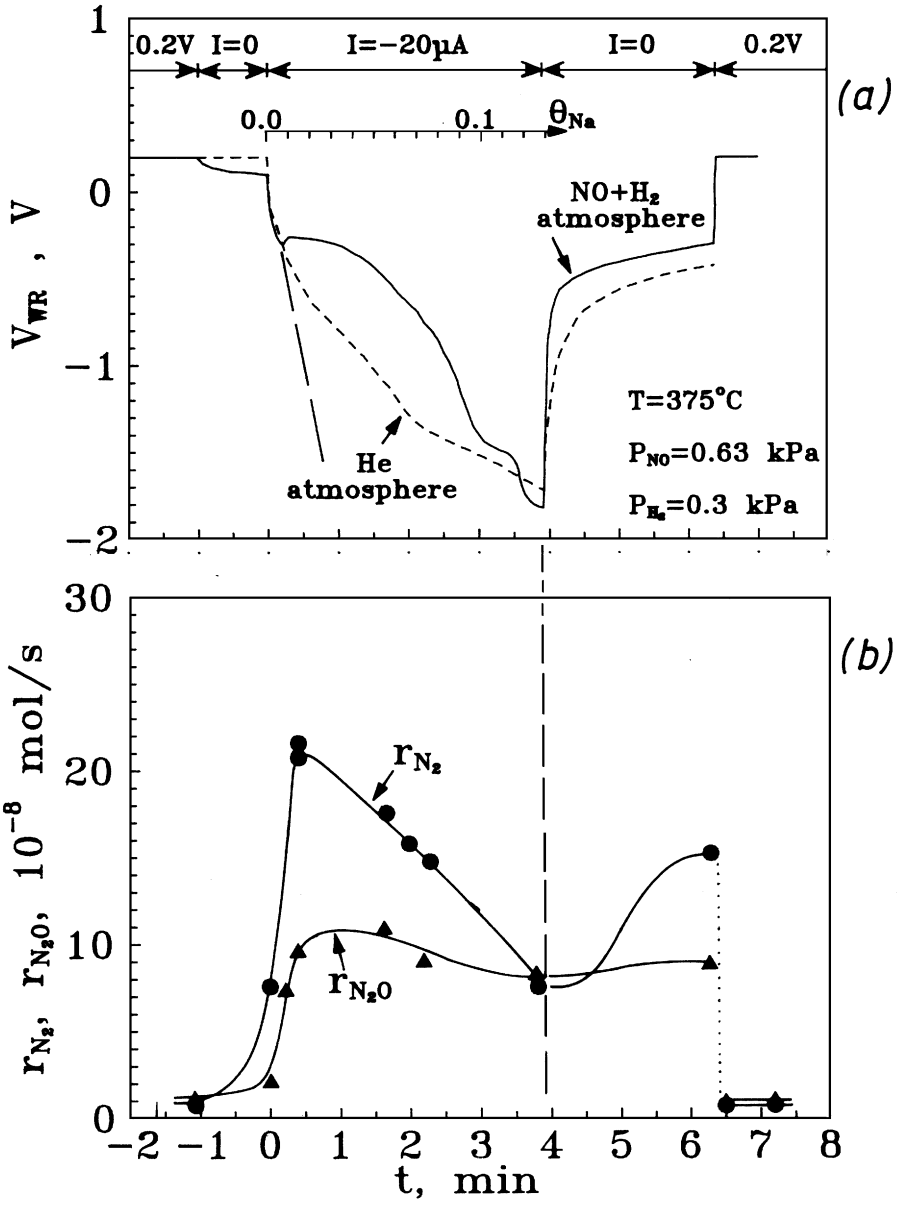

FIG. 3. Transient effect of applied constant negative current (Na supply to the catalyst) on catalyst potential (a) under reaction conditions (solid line) and in a He atmosphere (dashed line) and on the rates of formation of N_2 and N_2O (b). Potentiostatic restoration of the initial rates; see text for discussion.

value of 1.8×10^{-7} mol O is a factor of two smaller than that obtained by titration ($N_O = 3.8 \times 10^{-7}$ mol O).

Referring to Figs. 3a and 3b we first concentrate on the solid V_{WR} and rate and lines which correspond to an initial potentiostatically imposed value of 0.2 V ($t < -1$ min). The potentiostat is then disconnected ($I = 0$, $t = -1$ min) and V_{WR} relaxes to ~0.0 V, i.e., to the value imposed by the gaseous composition and corresponding surface coverages of NO and hydrogen. Similar to the steady-state results discussed below this decrease in catalyst potential from 0.2 to 0 V causes a six fold enhancement in the rate of N_2 formation and a 50% increase in the rate of N_2O formation. Then at $t = 0$ the galvanostat is used to impose a constant current $I = -20\ \mu$A; Na^+ is now pumped to the catalyst surface at a rate $I/F = 2.07 \times 10^{-10}$ mol Na/s. The corresponding Na coverage, θ_{Na}, starts increasing according to Eq. [2], causing a pronounced decrease in the catalyst potential V_{WR}, and thus (3) catalyst work function $e\Phi$, and a pronounced increase in the rate of N_2 and N_2O production, which go through a maximum when $V_{WR} \approx -0.5$ V. At this point r_{N_2} has increased by a factor of 20 with a significant enhancement in the selectivity to N_2. This transient behavior is qualitatively similar to the steady state rate vs V_{WR} behavior discussed below.

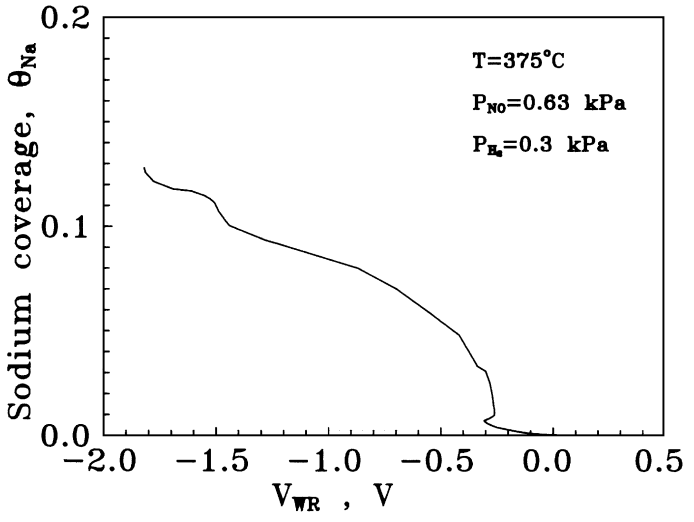

FIG. 4. Dependence of Na coverage on catalyst potential V_{WR} for the conditions of Fig. 3 ($P_{NO} = 0.63$ kPa, $P_{H_2} = 0.3$ kPa, $T = 375°C$).

Upon current interruption at $t = 4$ min, V_{WR} relaxes to -0.3 V, causing r_{N_2} and r_{N_2O} to return to their corresponding values at this potential during the previous galvanostatic transient. Potentiostatic imposition of the initial V_{WR} value ($= 0.2$ V) restores both rates to their initial, unpromoted, values showing the reversibility of the system (Fig. 3).

Steady-State Effect of Catalyst Potential

Figure 5 shows the steady-state effect of catalyst potential V_{WR} (Fig. 5a) and corresponding Na coverage, θ_{Na} (Fig. 5b), on r_{N_2} and r_{N_2O}, and on the selectivity to N_2 at 375°C and fixed partial pressures of NO and H_2, P_{NO}, and P_{H_2}, respectively. The selectivity to N_2, S_{N_2}, is defined as

$$S_{N_2} = r_{N_2}/(r_{N_2} + r_{N_2O}). \quad [5]$$

As previously noted, V_{WR} values above 0.2 V correspond to a Na-free catalyst surface. Decreasing V_{WR} and thus increasing θ_{Na} causes a dramatic enhancement in r_{N_2} and r_{N_2O}. The rate of N_2 formation, r_{N_2}, in particular increases by a factor of 30 at $V_{WR} = -0.6$ V. The rate enhancement ratio ρ_{N_2} defined as

$$\rho_{N_2} = r_{N_2}/r^o_{N_2}, \quad [6]$$

where $r^o_{N_2}$ is the unpromoted r_{N_2} value, is thus 30. This is the second largest (11) ρ value obtained in NEMCA studies with β''-Al_2O_3. The N_2O production rate increases by a factor of 6 and goes through a maximum with decreasing V_{WR}, thus increasing θ_{Na}. The selectivity to N_2, S_{N_2}, increases from 36% on the clean Pt surface to 75% for $V_{WR} = -0.6$ V ($\theta_{Na} = 0.06$).

Figure 5 demonstrates the strong promotional action of Na for the reduction of NO, the total rate of which increases by a factor of 14.5. The promotion index of Na, defined as

$$PI_{Na} = \frac{\Delta r_{NO}/r^o_{NO}}{\Delta\theta_{Na}}, \quad [7]$$

is as high as 6000 for low (<0.005) Na coverages (Fig. 5b), the second highest (11) value reported in NEMCA studies.

Effect of Gaseous Composition

Figures 6a and 6b show the effect of the hydrogen partial pressure, P_{H_2}, at constant P_{NO} on the rates of formation of N_2 and N_2O, respectively, at three fixed values of catalyst potential V_{WR}. For $V_{WR} = 0.4$ V the Pt surface is Na-free and both r_{N_2} (Fig. 6a) and r_{N_2O} (Fig. 6b) are low. Both rates exhibit a maximum at $P^*_{H_2} \approx 0.1$ kPa (hereafter denoting the P_{H_2} value which maximizes r_{N_2} and r_{N_2O}). Decreasing V_{WR} to 0.0 and -0.4 V, which corresponds to increasing the Na coverage to approximately 0.001 and 0.04 (Fig. 4), causes a pronounced increase in the rates and a shift of $P^*_{H_2}$ to 0.3 kPa. At this hydrogen partial pressure value, ρ_{N_2} and ρ_{N_2O} take the values of 11 and 6 for $V_{WR} = 0$ V and 18 and 11 for $V_{WR} = -0.4$ V. S_{N_2} is practically unaffected by P_{H_2} on the Na-free surface ($\approx 50\%$) and increases with P_{H_2} from 55 to 80% on the Na-promoted surface (Fig. 6c).

The dependence of r_{N_2} and r_{N_2O} on P_{NO} is shown in Figs. 7a and 7b for the same three fixed values of catalyst potential. Decreasing catalyst potential, and thus increasing Na coverage, causes again a pronounced increase in both r_{N_2} and r_{N_2O} and a decrease in the partial of NO, P_{NO}, which maximizes r_{N_2}. Note that r_{N_2O} develops a rate maximum only for $V_{WR} = -0.4$ V and that there is practically no difference in r_{N_2O} for $V_{WR} = 0.4$ and 0.0 V.

Increasing Na coverage enhances S_{N_2} over the entire P_{NO} range (Fig. 7c). The effect is more pronounced for intermediate P_{NO} values for which S_{N_2} exhibits a maximum as a function of P_{NO} (Fig. 7c).

Effect of Catalyst Potential on Activation Energies

Figures 8a and 8b show Arrhenius plots for r_{N_2} and r_{N_2O}, respectively, obtained at fixed P_{H_2} and P_{NO} and various fixed values of catalyst potential V_{WR}. These plots show again the very strong promotional effect on Na and the very high values of ρ_{N_2} and ρ_{N_2O} (up to 30 and 12, respectively).

The apparent activation energies for N_2 and N_2O formation, E_{N_2} and E_{N_2O}, respectively, are 12 and 13 kcal/mol on the Na-free Pt surface. Decreasing V_{WR} and thus increasing θ_{Na} causes pronounced changes in E_{N_2} and E_{N_2O} with the appearance of a break in the Arrhenius plots so that E_{N_2} and E_{N_2O} have two values each for every $V_{WR} \leq 0$. We denote these values as $E^{(I)}_{N_2}$, $E^{(I)}_{N_2O}$ and $E^{(II)}_{N_2}$, $E^{(II)}_{N_2O}$ for the high (I) and low (II) temperature range, respectively. Figure 9 shows the dependence of $E^{(I)}_{N_2}$, $E^{(II)}_{N_2}$, $E^{(I)}_{N_2O}$, and $E^{(II)}_{N_2O}$ on the catalyst potential V_{WR}. Both $E^{(II)}_{N_2}$ and $E^{(II)}_{N_2O}$ go through a maximum at $V_{WR} = -0.1$ V and then remain

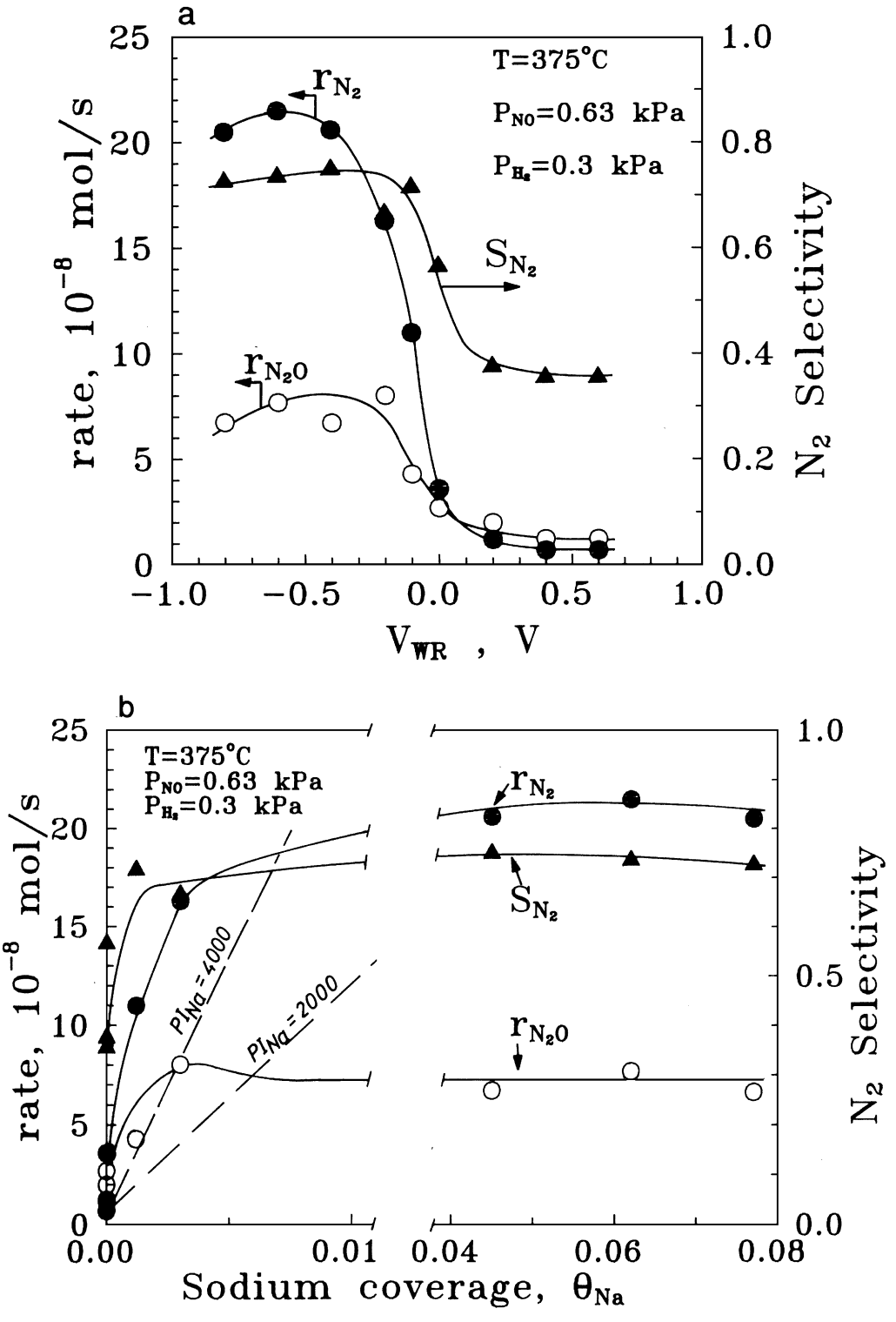

FIG. 5. Effect of catalyst potential (a) and corresponding Na coverage (b) on the rates of formation of N_2 and N_2O and on the selectivity to N_2.

practically stable at 22 and 8 kcal/mol, respectively, for more negative potentials. $E_{N_2}^{(I)}$ also goes through a maximum at $V_{WR} = 0$ V and then remains practically constant at 7 kcal/mol. $E_{N_2O}^{(I)}$ goes through a pronounced minimum at $V_{WR} = -0.1$ V and stabilizes to a constant negative value (-14 kcal/mol) for lower V_{WR} values.

Such activation energy maxima with V_{WR} have also been obtained in the NEMCA study of CO oxidation on

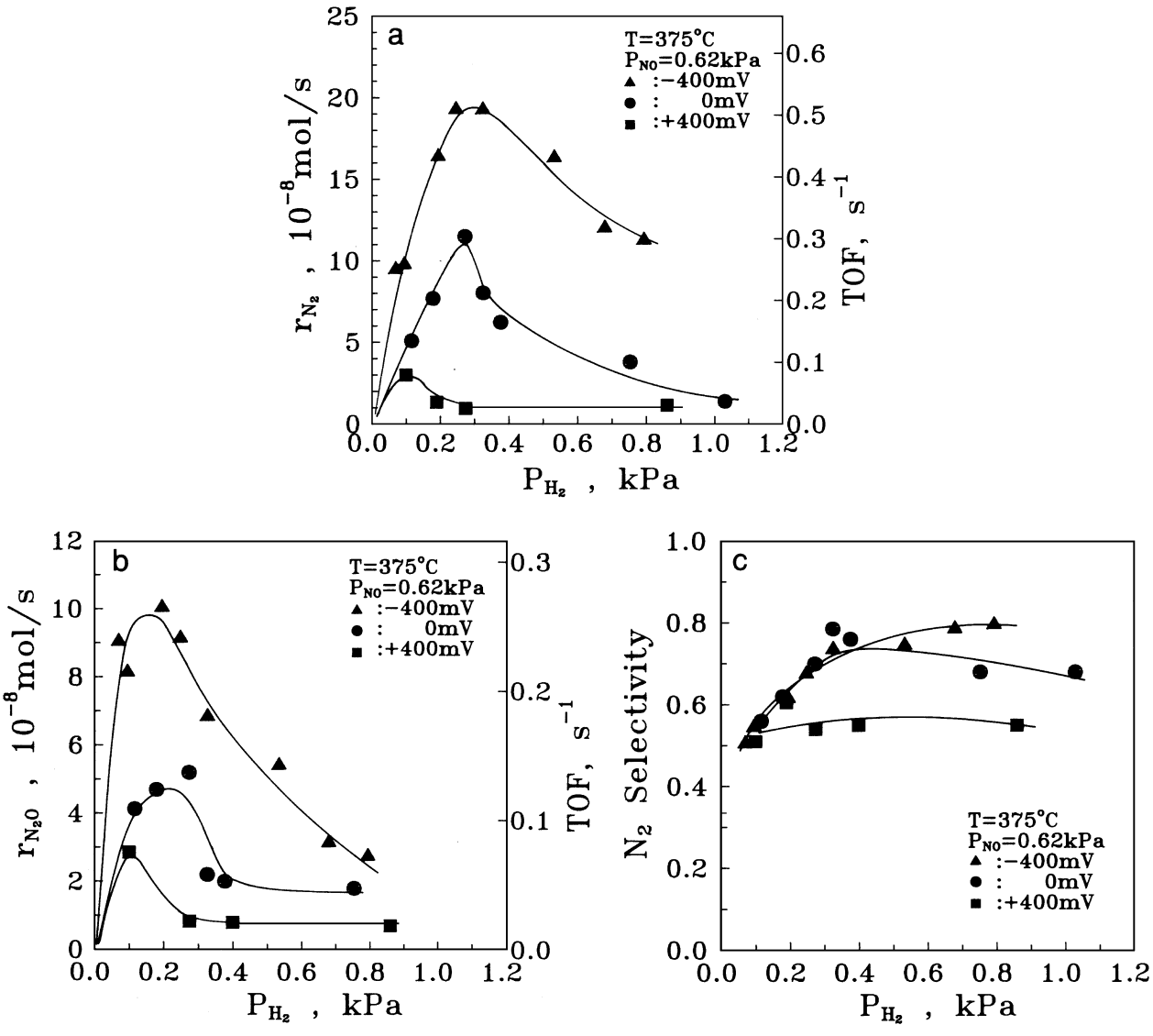

FIG. 6. Effect of P_{H_2} on the rates of formation of N_2 (a) and N_2O (b) and on selectivity to N_2 (c) for fixed P_{NO} and various fixed V_{WR} values.

Pt/β''-Al_2O_3 and have been explained quantitatively on the basis of Langmuir–Hinshelwood type kinetics by taking into account the variation of adsorption equilibrium constants with potential (12).

Figure 9a also shows the effect of V_{WR} on the temperature, T_b, of the break in the Arrhenius plots of r_{N_2} of r_{N_2O}. Decreasing V_{WR}, i.e., increasing Na coverage, decreases T_b for both reactions.

DISCUSSION

The present results show that the catalytic activity and selectivity of Pt for the NO reduction by H_2 can be altered dramatically and reversibly by dosing Na on the Pt catalyst surface. The measured values of the promotion index of Na, PI_{Na}, is up to 6000 for the rate of N_2 formation. Sodium enhances dramatically both the rate of NO reduction and the selectivity to N_2.

As in all previous electrochemical promotion studies of NO reduction on Pt, all the observed features can be explained by two factors:

1. Sodium enhances NO chemisorption vs H_2 chemisorption. This is apparent from the observed increase in $P^*_{H_2}$ and decrease in P^*_{NO} with increasing Na coverage (Figs. 6 and 7) and is consistent with the general rule used to rationalize all previous electrochemical promotion studies, i.e., that increasing coverage of electropositive promoters, and thus decreasing catalyst work function, strengthens the chemisorptive bond of electron acceptor adsorbates (e.g., NO) and weakens the chemisorptive bond of electron donor adsorbates (e.g., H).

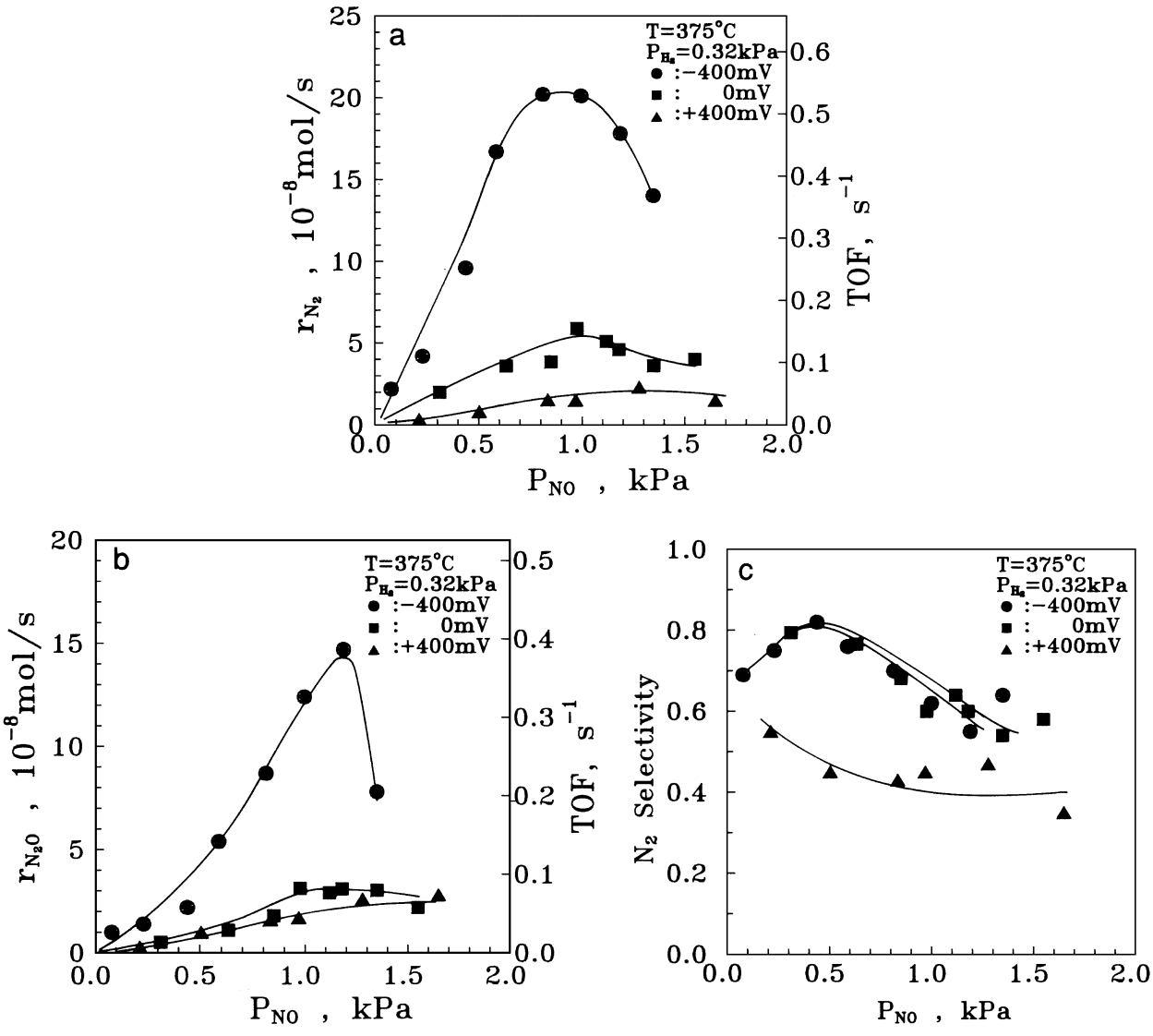

FIG. 7. Effect of P_{NO} on the rates of formation of N_2 (a) and N_2O (b) and on the selectivity to N_2 (c) for fixed P_{H_2} and various fixed V_{WR} values.

2. Sodium enhances NO dissociation on the Pt surface. This is a consequence of the first factor and is apparent from the observed dramatic enhancement in selectivity to N_2 with increasing Na coverage (Fig. 5).

One can thus rationalize all the observed features of the present study by considering the following reaction scheme:

$$NO(g) \leftrightharpoons NO(a) \quad [8]$$

$$NO(a) \leftrightharpoons N(a) + O(a) \quad [9]$$

$$NO(a) + N(a) \rightarrow N_2O(g) \quad [10]$$

$$N(a) + N(a) \rightarrow N_2(g) \quad [11]$$

$$H_2(g) \leftrightharpoons 2H(a) \quad [12]$$

$$2H(a) + O(a) \leftrightharpoons H_2O(g). \quad [13]$$

The role of H_2 is thus to scavenge atomic oxygen resulting from the NO dissociation step [9]. Increasing P_{H_2} decreases the coverage, θ_O, of atomic oxygen, thus increasing the ratio θ_N/θ_{NO} of the coverages of N and NO, respectively, according to the equilibrium [9] thus enhancing the selectivity to N_2 (Fig. 6c).

The enhanced chemisorption of NO vs H with decreasing V_{WR} is clearly manifested by observing the effect of V_{WR} on the kinetic behavior with respect to P_{H_2} (Figs. 6a and 6b) and with respect to P_{NO} (Figs. 7a and 7b). In the former case decreasing V_{WR} shifts the P_{H_2} value which maximizes the rate, $P^*_{H_2}$, to higher values, indicating a weakening in the chemisorptive bond of atomic hydrogen. In the latter case, decreasing V_{WR} causes the appearance of a rate

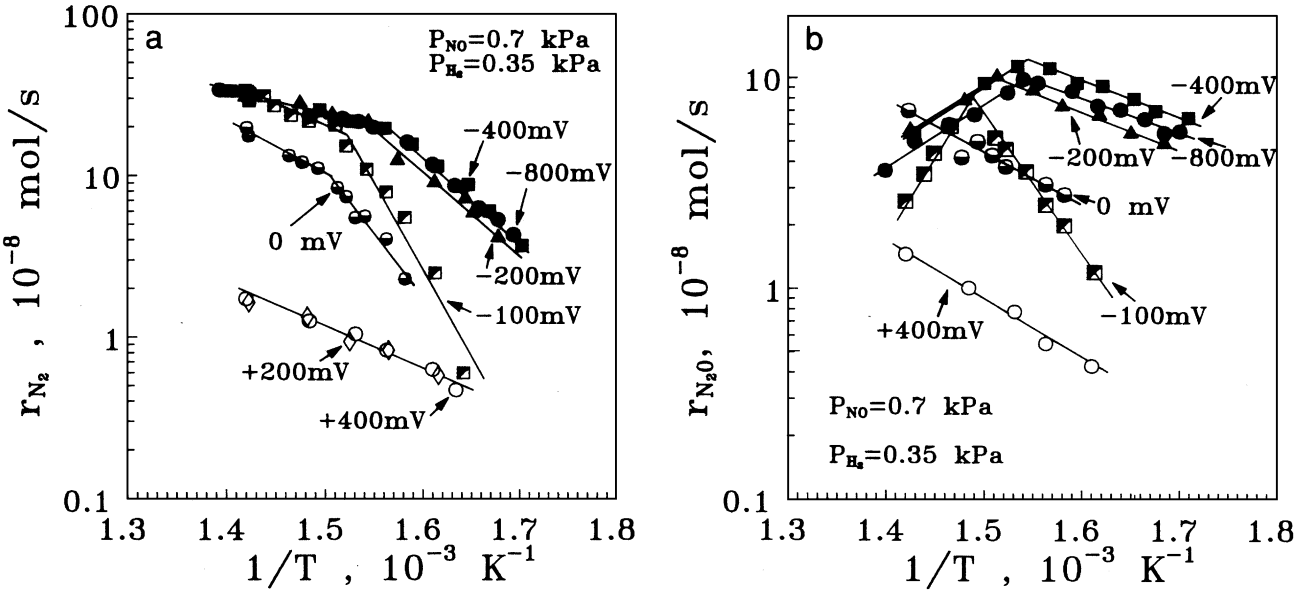

FIG. 8. Arrhenius plots of the rates of formation of N_2 (a) and N_2O (b) at various fixed V_{WR} values.

maximum with respect to P_{NO}, which shifts to lower values with decreasing V_{WR}, which shows a significant strengthening in the chemisorptive bond of NO. This strengthening in the chemisorptive bond of NO with decreasing V_{WR} leads eventually to extensive NO dissociation and this causes the observed pronounced enhancement in the selectivity to N_2 (Figs. 5a, 6c, and 7c).

The observed breaks in the Arrhenius plots (Figs. 8a and 8b) manifest the transition from a H-rich surface to a NO- and N-rich surface. Thus for the gaseous composition of the Arrhenius plots and for high V_{WR} values, both rates, r_{N_2} and r_{N_2O}, are first order in NO and negative order in H_2 (Figs. 6a and 7a). Under these conditions the surface, promoted at low T or unpromoted, is predominantly covered with atomic H. Upon decreasing V_{WR} both rates approach their maximum values (Figs. 6a and 7a) which indicates roughly equal coverages of H and NO on the surface. This, as analyzed below, causes a break in the Arrhenius plot and a decrease in the apparent activation energy with increasing T.

It is worth noting that decreasing V_{WR} causes a decrease in the temperature, T_b, of the break which is consistent with the enhanced NO (vs H) chemisorption with decreasing V_{WR} and with a higher heat of adsorption of hydrogen (vs NO) on the Pt surface. It is also worth noting that, for any fixed temperature, the V_{WR} value corresponding to the Arrhenius plot break is lower for r_{N_2} than for r_{N_2O} (Fig. 9, top). This is because decreasing V_{WR} increases the ratio θ_N/θ_{NO} which is proportional to the ratio r_{N_2}/r_{N_2O} according to the above reaction scheme [8] to [13].

After establishing that the observed breaks in the Arrhenius plots (Figs. 8a and 8b) are related to a change in the reaction orders with respect to NO and H_2, one can rationalize the observed behavior (Figs. 8 and 9) as follows:

In a previous paper (12) we analyzed the variation in apparent activation energy with temperature and different levels of promoters affecting the adsorption equilibrium constants for bimolecular Langmuir–Hinshelwood kinetics. The analysis was applied to the case of CO oxidation on Pt and was found to be in almost quantitative agreement with experiment (12). One can write more generally Eq. [18] of Ref. (12) for the apparent activation energy E of any simple bimolecular reaction,

$$A + B \rightarrow C, \qquad [14]$$

which follows Langmuir–Hinshelwood kinetics as

$$E = E_R - Q_A - Q_B + 2\frac{K_A P_A Q_A + K_B P_B Q_B}{1 + K_A P_A + K_B P_B}, \qquad [15]$$

where E_R is the true activation energy for the surface reaction between adsorbed A and B, Q_A and Q_B are the heats of adsorption of A and B, and K_A and K_B are the adsorption equilibrium constants of A and B, which are both temperature- and promoter-dependent. Thus E changes from $E_R + Q_A + Q_B$ at low temperatures ($K_A P_A$, $K_B P_B \gg 1$) to $E_R - Q_A - Q_B$ at high temperatures ($K_A P_A$, $K_B P_B \ll 1$) and can easily become negative. If the rate is at the maximum ($K_A P_A \approx K_B P_B$) and reactant adsorption is strong ($K_A P_A \gg 1$), then it follows from Eq. [15] that $E = E_R$.

In the present case the situation is more complex to analyze due to the surface NO dissociation step. By analogy to the above analysis for the reaction scheme [8] to [13] one may conclude that differences $E^{(II)}_{N_2} - E^{(I)}_{N_2}$ and $E^{(II)}_{N_2O} - E^{(I)}_{N_2O}$

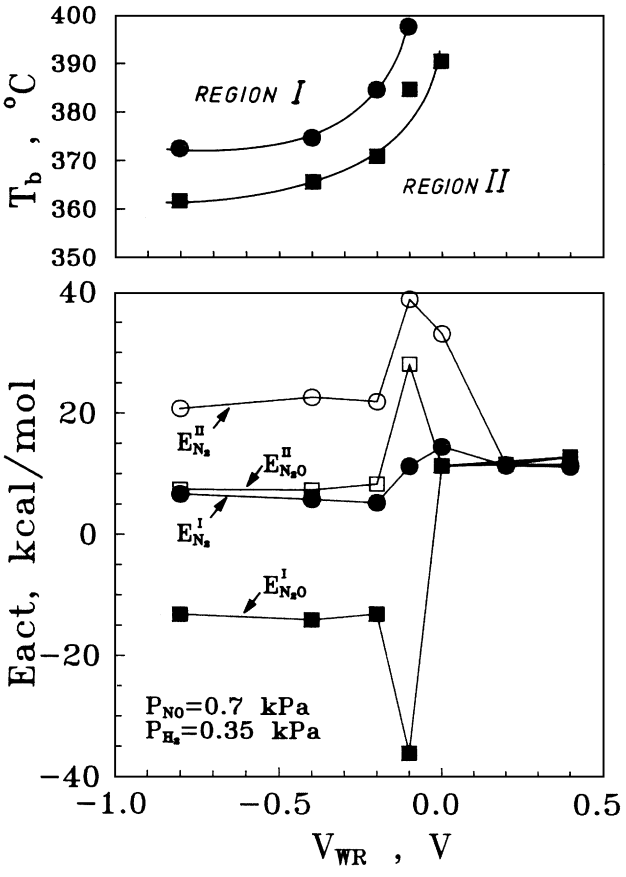

FIG. 9. Effect of catalyst potential V_{WR} on the temperature of the break in the Arrhenius plots, T_b (top), and on the activation energies of r_{N_2} (circles) and r_{N_2O} (squares) in the high T (I) and low T (II) ranges, respectively.

(16 and 19 kcal/mol, respectively) relate to the heat of adsorption of hydrogen, while the difference $E^{(I)}_{N_2} - E^{(I)}_{N_2O}$ and $E^{(II)}_{N_2} - E^{(II)}_{N_2O}$ (20 and 15 kcal/mol, respectively) relates to the activation energy for NO dissociation on the promoted Pt surface.

The very similar values of the activation energies for both reactions on the unpromoted surface (Figs. 8a and 8b) indicate that in this case both rates are probably controlled by the same rate limiting reaction,

$$H + NO \rightarrow N + OH, \qquad [16]$$

followed by rapid reaction of OH with H to form H_2O. Under these conditions the extent of NO dissociation must by very small and the nondissociative mechanism must be dominant.

In conclusion the observed very pronounced promotional role of Na for this reaction system can be mainly attributed to the pronounced enhancement of NO dissociation (step [9] of the reaction scheme). The ability of solid electrolytes to tune precisely the coverage of promoters on catalyst surfaces is of considerable theoretical and practical importance.

ACKNOWLEDGMENTS

We thank the CEC JOULE Programme and the EPET II and PENED Programmes of the Hellinic Secretariat of Research and Technology for partial financial support.

REFERENCES

1. Vayenas, C. G., Bebelis, S., and Neophytides, S. G., *J. Phys. Chem*. **92**, 5083 (1988).
2. Bebelis, S., and Vayenas, C. G., *J. Catal.* **118**, 125 (1989).
3. Vayenas, C. G., Bebelis, S., and Ladas, S., *Nature (London)* **343**, 625 (1990).
4. Politova, T. I., Sobyanin, V. A., and Belyaev, V. D., *React. Kinet. Catal. Lett.* **41**, 321 (1990).
5. Vayenas, C. G., Bebelis, S., and Despotopoulou, M., *J. Catal.* **128**, 415 (1991).
6. Cavalca, C. A., Larsen, G., Vayenas, C. G., and Haller, G. L., *J. Phys. Chem*. **97**, 6115 (1993).
7. Mar'ina, O. A., Sobyanin, V. A., Belyaev, V. D., and Parmon, V. N., *Catal. Lett.* **13**, 567 (1992).
8. Varkaraki, E., Nicole, J., Plattner, E., Comninellis, Ch., and Vayenas, C. G., *J. Appl. Electrochem*. **25**, 978 (1995).
9. Pliangos, C., Yentekakis, I. V., Verykios, X. E., and Vayenas, C. G., *J. Catal.* **154**, 124 (1995).
10. Pritchard, J., *Nature (London)* **342**, 592 (1990).
11. Harkness, I. R., and Lambert, R. M., *J. Catal.* **152**, 211 (1995).
12. Yentekakis, I. V., Moggridge, G., Vayenas, C. G., and Lambert, R. M., *J. Catal.* **146**, 292 (1994), and references therein.
13. Cavalca, C. A., and Haller, G. L., *J. Catal.*, in press (1996).
14. Vayenas, C. G., Bebelis, S., Yentekakis, I. V., and Lintz, H.-G., *Catal. Today* **11**, 303 (1992).
15. Vayenas, C. G., Ladas, S., Bebelis, S., Yentekakis, I. V., Neophytides, S., Jiang,Yi, Karavasilis, Ch., and Pliangos, C., *Electrochim. Acta* **39**, (11/12), 1849 (1994).
16. Vayenas, C. G., Jaksic, M. M., Bebelis, S. I., and Neophytides, S. G., The electrochemical activation of catalytic reactions, *in* "Modern Aspects of Electrochemistry" (J. O' M. Bockris, B. E. Conway, and R. E. White, Eds.), Vol. 29, pp. 57–202. Plenum, New York, 1995.
17. Vayenas, C. G., and Yentekakis, I. V., Electrochemical Modification of Catalytic Activity, *in* "Handbook of Heterogeneous Catalysis" (G. Ertl, H. Knötzinger, and J. Weitkamp, Eds.), in press. VCH Publishers, 1997.
18. Bebelis, S., and Vayenas, C. G., *J. Catal.* **138**, 570 (1992).
19. Neophytides, S., and Vayenas, C. G., *J. Phys. Chem*. **99**, 17063 (1995).
20. Tsiplakides, D., Neophytides, S., Enea, O., Jaksic, M. M., and Vayenas, C. G., *J. Electrochem. Soc.*, in press (1997).
21. Makri, M., Buekenhoudt, A., Luyten, J., and Vayenas, C. G., *Ionics* **2** (1996).
22. Neophytides, S. G., Tsiplakides, D., Stonehart, P., Jaksic, M. M., and Vayenas, C. G., *Nature (London)* **370**, 45 (1994).
23. Palermo, A., Lambert, R. M., Harkness, I. R., Yentekakis, I. V., Mar'ina, O. A., and Vayenas, C. G., *J. Catal.* **161**, 471 (1996).
24. Lambert, R. M., Tikhov, M., Palermo, A., Yentekakis, I. V., and Vayenas, C. G., *Ionics* **1**, 366 (1995).
25. Palermo, A., Tikhov, M. S., Filkin, N. C., Lambert, R. M., Yentekakis, I. V., and Vayenas, C. G., *Stud. Surf. Sci. Catal.* **101**, 513 (1996).
26. Masel, R. I., *Catal. Rev.* **28**, 335 (1986).
27. Stenger, H. G., Jr., and Hepburn, J. S., *Energ. Fuels* **1**, 412 (1987).
28. Halasz, I., Brenner, A., and Shelef, M., *Catal. Lett.* **18**, 289 (1993).

29. Yentekakis, I. V., Pliangos, C. A., Papadakis, V. G., Verykios, X. E., and Vayenas, C. G., *in* "Catalysis and Automotive Pollution Control III. Vol. 96. Studies in Surface Science and Catalysis" (A. Frennet and J.-M. Bastin, Eds.), p. 375. Elsevier, Amsterdam, 1995.
30. Engler, B. H., Lindler, D., Lox, E. S., Schäfer-Sindlinger, A., and Ostgathe, K., *in* "Catalysis and Automotive Pollution Control III. Vol. 96. Studies in Surface Science and Catalysis" (A. Frennet and J.-M. Bastin, Eds.), p. 441. Elsevier, Amsterdam, 1995.
31. Masel, R. I., *Catal. Rev. Sci. Eng.* **28**, 335 (1986).
32. Gohndrone, J. M., and Masel, R. I., *Surf. Sci.* **209**, 44 (1989).
33. Zemlyanov, D. Y., Smirnov, M. Y., Gorodetskii, V. V., and Block, J. M., *Surf. Sci.* **329**, 61 (1995).
34. Kiskinova, M.P., *in* "Studies in Surface Science and Catalysis," Vol. 70, Sect. 6.3. Elsevier, Amsterdam, 1992.
35. Harkness, I. R., Hardacre, C., Lambert, R. M., Yentekakis, I. V., and Vayenas, C. G., *J. Catal.* **160**, 19 (1996).
36. Cavalca, C., Ph.D. thesis, Yale Univ., 1995.
37. Makri, M., Vayenas, C. G., Bebelis, S., Besocke, K., and Cavalca, C., *Surf. Sci.* **369**, 351 (1996).
38. Mikheeva, E. P., Devyatov, V. G., and Kolchanova, V. M., *Kinet. Katal.* **24**, 418 (1983).
39. Kolchanova, V. M., and Mikheeva, E. P., *React. Kinet. Catal. Lett.* **24**, 207 (1984); **26**, 339 (1984).
40. Ladas, S., Bebelis, S., and Vayenas, C. G., *Surf. Sci.* **251/252**, 1062 (1991).
41. Hölzl, J., and Schulte, F. K., *in* "Solid Surface Physics" (G. Höhler and E. Niekisch, Eds.), pp. 1–150. Springer-Verlag, Berlin, 1979.
42. Gundry, P. M., and Tompkins, F. C., *in* "Experimental Method in Catalytic Research" (R. B. Anderson, Eds.), pp. 100–168. Academic Press, NY, 1968.
43. Pirug, G., and Bonzel, H. P., *J. Catal.* **50**, 64 (1977).